processes

MDPI

Article

Synthesis of Palladium and Copper Nanoparticles Supported on TiO_2 for Oxidation Solvent-Free Aerobic Oxidation of Benzyl Alcohol

Hamed M. Alshammari

Chemistry Department, Faculty of Science, Ha'il University, Ha'il P.O. Box 2440, Saudi Arabia;
h.alshammari@uoh.edu.sa

Abstract: The use of metal oxides as supports for palladium and copper (Pd–Cu) nanoalloys constitutes a new horizon for improving new active catalysts in very important reactions. From the literatures, Pd-based bimetallic nanostructures have great properties and active catalytic performance. In this work, nanostructures of titanium dioxide (TiO_2) were used as supports for Pd–Cu nanoparticles catalysts. Palladium and copper were deposited on these supports using the sol-immobilisation method. The composite nanoalloys were characterized using transmission electron microscopy (TEM) and X-ray photoelectron spectroscopy (XPS). The catalyst was evaluated for the oxidation of benzyl alcohol. The effect of the Cu–Pd ratio using sol-immobilization methods supported on TiO_2 was investigated. The results show that monometallic Cu/TiO_2 was observed to have a low activity. However, as soon as the catalyst contained any palladium, the activity increased with a significant increase in the selectivity towards isomerization products. The influence of support and temperature were investigated. Furthermore, the catalyst reusability was also tested for oxidation of benzyl alcohol reactions, by repeatedly performing the same reaction using the recovered catalyst. The $Pd–Cu/TiO_2$ catalyst displayed better reusability even after several reactions

Keywords: Pd–Cu bimetallic catalyst; benzyl alcohol; TiO_2; oxidation of alcohol

check for updates

Citation: Alshammari, H.M. Synthesis of Palladium and Copper Nanoparticles Supported on TiO_2 for Oxidation Solvent-Free Aerobic Oxidation of Benzyl Alcohol. *Processes* **2021**, *9*, 1590. https://doi.org/10.3390/pr9091590

Academic Editor: Sónia Carabineiro

Received: 19 July 2021
Accepted: 2 September 2021
Published: 5 September 2021

1. Introduction

The oxidation of alcohols is an important chemical reaction for the synthesis of aldehydes, which are useful intermediaries and final products for several pharmaceutical, perfume, beverage, and agrochemical industries [1–4]. Carbonyl compounds are also important products of oxidation of alcohols, used in the synthesis of new molecules.

The selective oxidation of alcohols is important for research carried out in academic laboratories as well as in industry research and development. It is a common approach for the synthesis of different carbonyl compounds [5].

Benzyl alcohol has been studied extensively as a substrate of many reactions [6–8]. Oxidation of benzyl alcohol produces benzaldehyde, which is a valuable intermediate and has several applications in the synthesis of fine chemicals, pharmaceutical and agrochemical products, flavouring additives and fragrances [6,9,10]. Strong oxidizing agents, such as potassium permanganate and dichromate, are used in industries to produce benzaldehyde due to the feasibility of controlling the reaction conditions with high yield [11,12]. However, these oxidants are not the most suitable reagents for industries as they can, due to their toxic nature, cause serious environmental damage, and, in addition, because of their high cost [13–15].

Over the last few decades, heterogenous precious metals catalysts, such as palladium (Pd), platinum (Pt), gold (Au) and ruthenium (Ru), have been used as monometallic catalysts in the selective oxidation of benzyl alcohol and the synthesis of benzaldehyde [16–20]. Heterogenous catalysis is one of the key processes for fabrication of chemicals in industries and an important process for the sustainable future of energy industries [21,22]. Metal nanoparticles (NPs) are likely candidates for catalysis in comparison to bulk metals due to their superior catalytic activities and increased surface area per volume, exhibited by heterogenous metal-NPs, which typically work on metal surfaces [23]. Pd is a paramagnetic metal that is used in organic reactions, whereas Pd NPs are ferromagnetic and exhibit high catalysis in hydrogenation and hydrolysis reactions [24–26]. Studies suggest that the activity of catalysis can be linked to the metal loading and choice of support system in the catalyst preparation, which determines selective reactivity. For Pd NPs, the most common types of support used are Al_2O_3, SiO_2 and TiO_2 [27]. TiO_2 is extensively applied as catalyst support due to its high oxygen storage capacity, redox property and metal dispersion ability [28]. TiO_2 also exhibits many beneficial properties and is widely used in different industries as a catalyst support [29]. The TiO_2 nanoparticles are covered by hydroxyl moieties. The main amphoteric surface function group is the titanol (TiOH) moiety, which undergoes the acid–base equilibrium [29]. The acid–base interactions between the surface and entering reactants can result in the formation of activated complexes, which can then drive the reactions.

Bimetallic NPs include two different metals, and their synergistic effect results in unique chemical and physical properties, leading to enhanced catalytic function, improves product selectivity and suppression of catalytic deactivation. On the basis of these concerns, it may be worthwhile to support the use of bimetallic NPs on the TiO_2. The combination of Pd and Cu as a bimetallic catalyst is extensively used in various chemical reactions [20–31]. However, the high cost and the limited availability of noble metals requires special support to decrease the percentage of noble metals used. The use of such supports may reduce the overall cost of the production, as well as the quantity of catalyst used [32–34]. Therefore, the selection of suitable supports for a Pd–Cu bimetallic catalyst is essential for the oxidation of benzyl alcohol.

The influence of TiO_2-supported Pd–Cu has not been sufficiently tested, to date. Hence, the present work investigated the catalytic performance of benzyl alcohol oxidation in an aqueous solution over Pd–Cu bimetallic supported on anatase.

2. Materials and Methods

2.1. Preparation of Catalyst

The sol-immobilisation technique was used to prepare bimetallic catalysts, supported on TiO_2. Aqueous solutions of $PdCl_2$ (Johnson Matthey, UK, 6 mg in 1 mL) and $CuCl_2$-$2H_2O$ (Johnson Matthey, 6 mg in 1 mL) were used to prepare 1 wt% of the Cu:Pd catalyst (1% Pd/TiO_2, 1% Cu/TiO_2, 0.75Pd-0.25Cu/TiO_2, 0.25Pd-0.75Cu/TiO_2, and 0.5Pd-0.5Cu/TiO_2). Cu and Pd solutions were mixed and prepared by stirring in 800 mL distilled water for 15 min. While stirring this solution for another 15 min, 1 wt% solution of polyvinyl alcohol (PVA) (Mw = 10,000, 80% hydrolyzed) was also added. Freshly prepared sodium borohydride solution (0.1 M, $NaBH_4$/Pd–Cu, mol/mol = 5) was added and then stirred continuously for 30 min, resulting in a dark brown solution. In this method, 1.98 g of the TiO_2 support was added and solution was stirred for 1 h. Recovery of catalyst was facilitated via filtration followed by washing with 2 L deionized water and drying at 110 °C for about 10 h.

2.2. Catalytic Performance

Benzaldehyde was obtained from the liquid phase oxidation of benzyl alcohol in a Radleys carousel reactor, using 50 mL glass stirred reactor. Under solvent-free conditions, two hundred milligrams of the TiO_2 supported Cu–Pd catalyst was dispersed in substrate (2 g). At a constant pressure of 1 bar, the mixture was stirred at 1000 rpm. Gas chromatography (Varian star CP-3800), which included a CP-wax 52 column as well as a flame ionization detector, was used to analyze a sample from this reaction mixture.

2.3. Catalyst Recyclability

The reusability of the bimetallic supported catalyst (0.5% Cu-0.5% Pd/TiO_2) was analyzed by separating the catalyst from the reaction mixture. The catalyst was suspended in acetone to remove the organic products and then separated by simple filtration. The isolated catalyst was dried for 1 h at 120 °C. After each cycle, the catalyst was collected by similar method and reused for the subsequent cycles.

2.4. Catalyst Characterization

XPS was collected on K-ALPHA (Themo Fisher Scientific, USA) with monochromatic X-ray Al K-alpha radiation -10 to 1350 e.V spot size 400 micro at pressure 10^9 mbar with full spectrum pass energy 200 e.V and at narrow spectrum 50 e.V. High-resolution transmission electron microscopy (HRTEM) pictures are taken using a JEOL model 2100 apparatus operating at 200 kV.

3. Results and Discussion

3.1. Materials Charcterization

The crystallite sizes and morphologies of the prepared catalysts were examined using TEM. Figure 1 depicts the morphology and textural characteristics of the developed catalysts. The catalyst particles are nano-sized, with stretched and asymmetric spherical forms, and were only weakly aggregated, according to TEM images. It was observed that some of the stretched particles had cubic shapes. Cu, Pd-loaded TiO_2 displayed almost spherical particles, with sizes ranging from 5 to 15 nm. The metals are most likely occupying substitutional sites on the TiO_2 lattice, as no particles were found on the surface of TiO_2. Moreover, it is obvious from the TEM images that the Cu- or Pd-promoted catalysts had fewer particles than pure TiO_2. These findings suggest that various metals have varying impacts on the entire size and structure of crystallites in the synthesized catalysts. HRTEM images revealed that the anatase TiO_2 surface had a disorderly layer with a thickness of 2–5 atomic layers. The selected area electron diffraction (SAED) was applied to confirm the anatase's local crystal structure. Figure 1 displays SAED ring diffraction pattern of the TiO_2 anatase. The ring pattern revealed that the nanopowder was polycrystalline, with individual crystallites ranging in size from 5 to 15 nanometers. Surprisingly, a few other lattice planes showed faint signals on the pattern, which were generated by the nanocrystals' randomization distribution.

Figure 2 displays the X-ray diffraction patterns of 1% Pd/TiO_2, 1% Cu/TiO_2, 0.75Pd-0.25Cu/TiO_2, 0.25Pd-0.75Cu/TiO_2, and 0.5Pd-0.5Cu/TiO_2. Pure anatase TiO_2 (JCPDS # 01-075- 2545) is observed in all samples indicating that its crystallinity is not affected by presence of Pd and Cu NPs. The absence of the Pd and Cu NPs was also demonstrated by the pattern. Besides, upon increase of the Cu content, an increase on the intensities of anatase peaks was observed.

To estimate the actual concentrations of Pd and Cu deposited on the TiO_2, the ICP-OES was performed. The actual bulk metallic concentrations were found to be smaller than the theoretical values, which could be due to weakly attached Cu–Pd bimettalic leaching during the preparation process.

XPS analysis were used to examine further the surface oxidation state of 1% Pd/TiO_2, 1% Cu/TiO_2, 0.75Pd-0.25Cu/TiO_2, 0.25Pd-0.75Cu/TiO_2 and 0.5Pd-0.5Cu/TiO_2 with the findings displayed in Figure 3 and the XPS data are presented in Table 1. The survey spectrum in Figure 3 shows that the elements of C, O, Ti, Cu and Pd make up the primary peaks of the prepared catalysts.

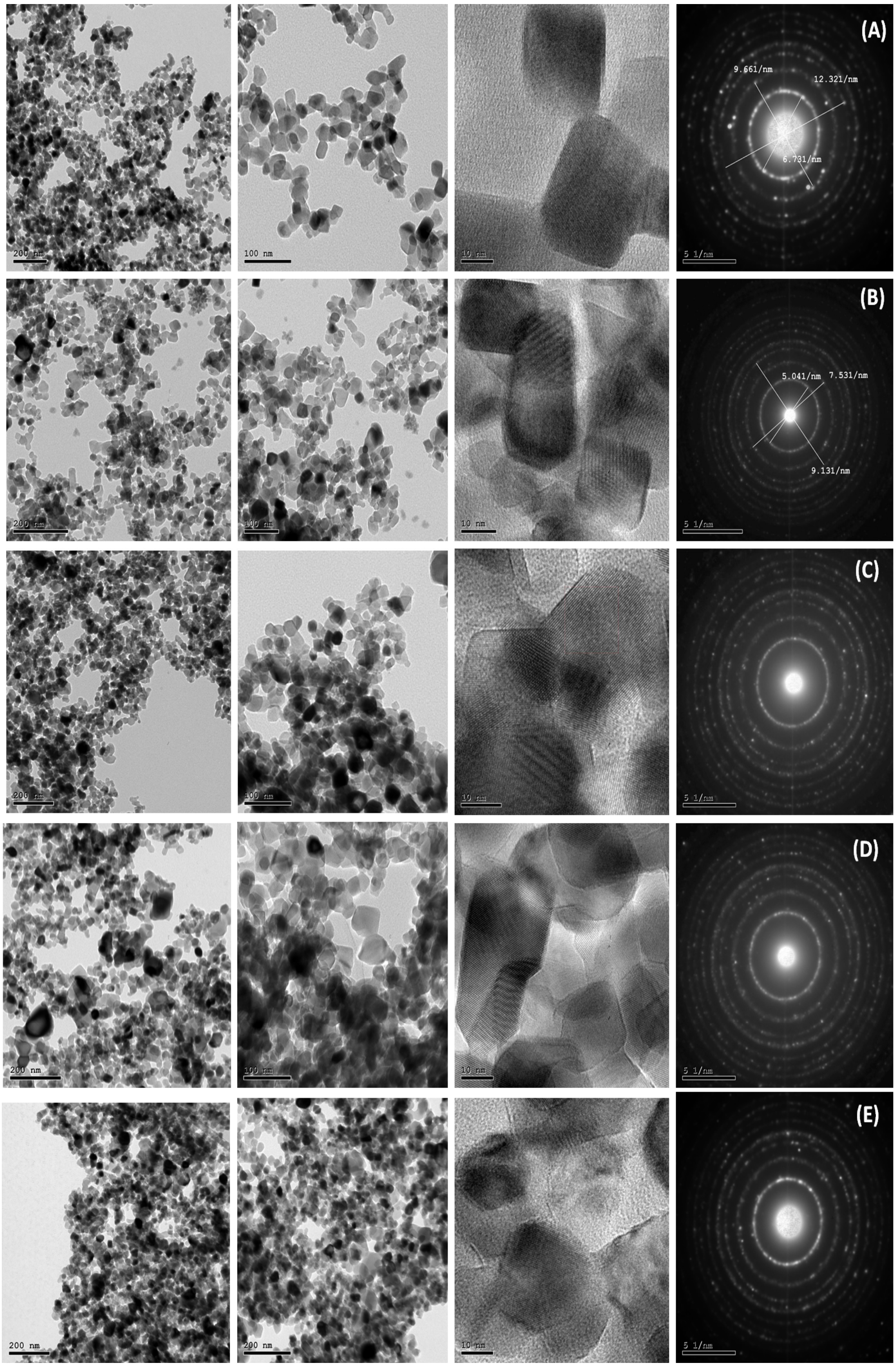

Figure 1. TEM, HRTEM images and SAED patterns of (**A**) 1% Pd/TiO_2, (**B**) 1% Cu/TiO_2, (**C**) 0.75Pd-0.25Cu/TiO_2, (**D**) 0.25Pd-0.75Cu/TiO_2 (**E**) 0.5Pd-0.5Cu/TiO_2.

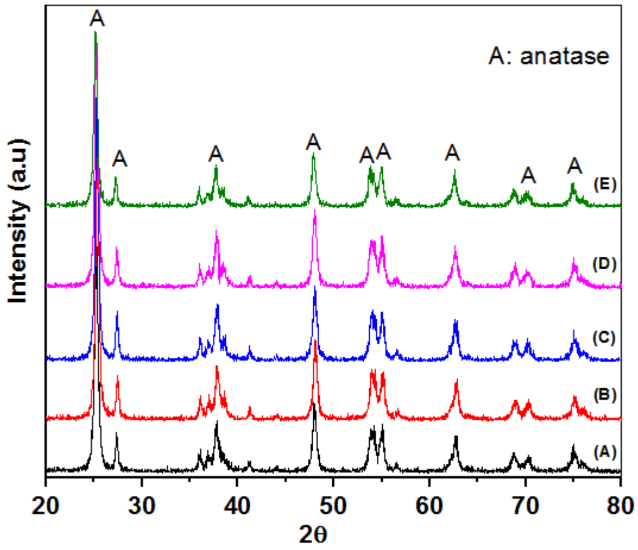

Figure 2. X-ray diffraction patterns of (**A**) 1% Pd/TiO_2, (**B**) 1% Cu/TiO_2, (**C**) 0.75Pd-0.25Cu/TiO_2, (**D**) 0.25Pd-0.75Cu/TiO_2 (**E**) 0.5Pd-0.5Cu/TiO_2.

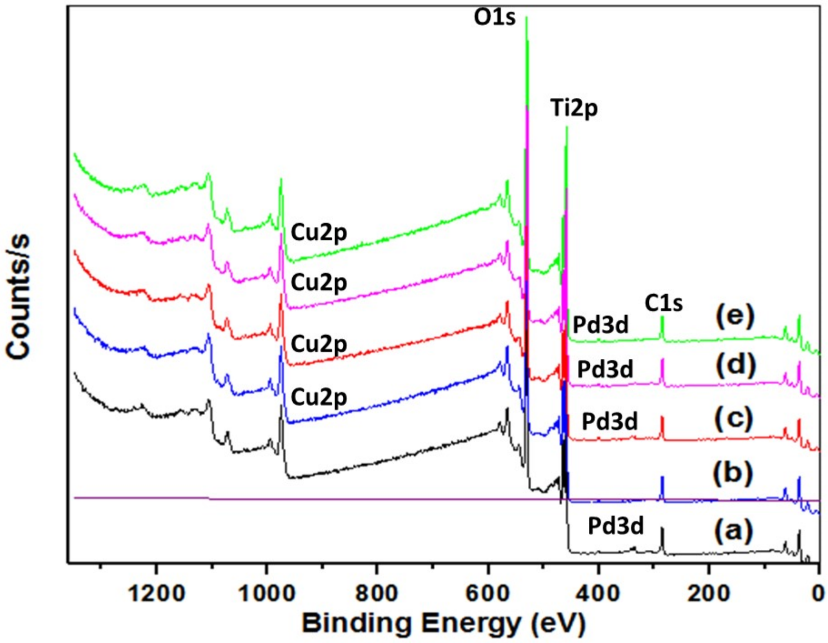

Figure 3. XPS survey spectrum of the prepared catalysts (**a**) 1% Pd/TiO_2, (**b**) 1% Cu/TiO_2, (**c**) 0.75Pd-0.25Cu/TiO_2, (**d**) 0.25Pd-0.75Cu/TiO_2 (**e**) 0.5Pd-0.5Cu/TiO_2.

Figure 4 illustrates a high-resolution XPS spectrum of a selected sample of 0.5Pd-0.5Cu/TiO_2 catalyst. The concentration of the chemical species at the surfaces are presented in Table 1. Figure 4a displayed the XPS spectrum of O 1s. At 529.7 eV, a definite peak occurred is observed, which can be attributed to O^{2-} in Ti-O nanoparticles. O_2, on the surface, recognizes one weak O 1s peak at 531.1 eV. Orbit-splitting produced the doublet, $Ti2p_{1/2}$ (464.1 eV) and $Ti2p_{3/2}$ (458.3 eV). These peaks correspond to Ti^{4+} in the TiO_2 lattice (Figure 4b). The produced catalyst's Pd 3d XPS spectrum (Figure 4c) demonstrates that the sample exhibited two duplicates of Pd $3d_{5/2}$ and Pd $3d_{3/2}$. The low-energy Pd $3d_{5/2}$ was resolved into Pd° and Pd^{2+}-related doublets at 334.9 and 336.7 eV. Pd $3d_{3/2}$ deconvolution yielded two peaks at 340.2 and 340.8 eV that are related to Pd ° and Pd^{2+}, respectively. Figure 4d shows the high-resolution Cu 2p spectrum, which is divided into Cu 2p3/2 and Cu 2p1/2 at 934.1 eV and 954.7 eV, respectively. The difference in energy between these two Cu 2p peak locations is 20.5 eV, which is substantially different from the preceding CuO spectra. Furthermore, the extended satellite peaks have a higher binding energy than the original peaks, indicating that CuO has been confirmed. Two bands at roughly 943.1 eV and 940.3 eV on the higher binding energy side followed the primary peak of Cu 2p3/2 at 934.1 eV, suggesting the presence of CuO [35–37]. Table 1 shows the surface atomic composition acquired from the XPS data. When compared to the Pd–Cu bulk concentration obtained by ICP-OES, the concentration of Pd and Cu on the Pd–Cu/TiO_2 surface was found to be lower than that in the bulk.

Table 1. Binding energies and surface contributions of Ti2P, O1S, Pd3d and Cu2p of and to the catalysts.

Sample	Ti2P [a]	O 1S [a]	Pd3d [a]	Cu2p [a]	Actual At.(%) Pd [b]	Actual At (%) Cu [b]
1%Pd/TiO_2	459.24 (23.34)	530.8 (55.64)	336.1 (0.41)	-	0.87	-
1% Cu/TiO_2	459.27 (22.81)	530.8 (57.69)	-	921.2 (0.25)	-	0.91
0.75Pd-0.25Cu/TiO_2	459.33 (21.05)	530.9 (55.4)	335.8 (0.27)	933.2 (0.07)	0.64	0.22
0.25Pd-0.75Cu/TiO_2	459.28 (20.84)	530.9 (58.61)	335.5 (0.17)	938.1 (0.21)	0.21	0.69
0.5Pd-0.5Cu/TiO_2	459.24 (20.67)	530.7 (54.47)	335.7 (0.39)	937.1 (0.22)	0.43	0.46

[a] The value between brackets represents the atomic % of the element; [b] the atomic percentage of Pd and Cu elements as determine from ICP-OES.

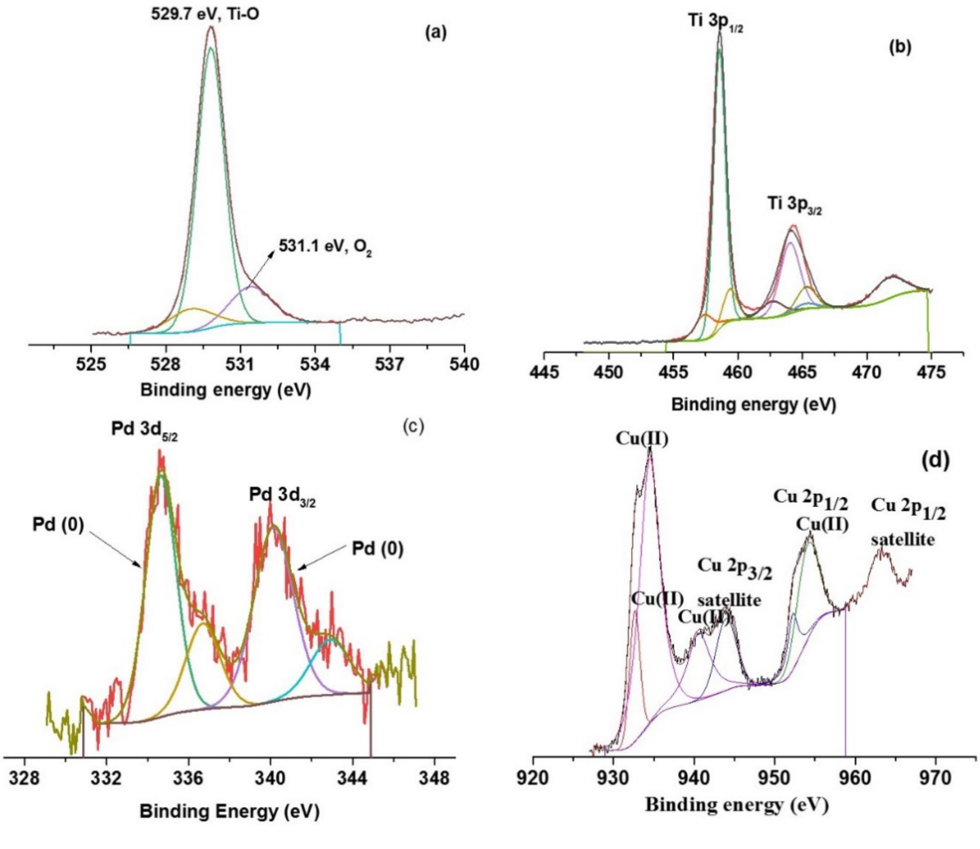

Figure 4. Core level XPS spectra of 0.5Pd-0.5Cu/TiO_2 (**a**) O 1s, (**b**) Ti3p, (**c**) Pd3d, and (**d**) Cu 2p.

3.2. *Catalytic Activity*

3.2.1. Effect of Cu–Pd Ratio Supported on TiO_2

Different ratio compositions of monometallic Cu and Pd catalysts and a bimetallic Cu–Pd catalyst with TiO_2 supports were used for the oxidation of benzyl alcohol at 120 °C under aerobic and solvent-free conditions. The performance of these catalysts, as well as selectivity of the major product benzaldehyde, are shown in Table 2 and the GC profiles were presented in (Supporting Information, Section S1). TiO_2 with 1 wt% copper nanoparticles showed poor activity but the best selectivity to benzaldehyde (99.9%), corresponding to TOF of 0.708 h^{-1} and TON of 0.354. Adding the Pd lead to a proportional increase in catalytic activity, with a broad maximum at 0.75Pd-0.25Cu/TiO_2 of 92% conversion with 96.2% selectivity of benzaldehyde corresponding to TOF of 263.81 h^{-1} and TON of 131.95. Increasing Pd content in the monometallic Pd/TiO_2 (1 wt%) showed smaller catalytic activity (92.2% conversion with 88.3% selectivity of benzaldehyde corresponding to TOF of 196.51 h^{-1} and TON of 193.02) than the catalyst containing 0.75% Pd. Based on major product selectivity, an increase in Pd content led to a slight decrease in aldehyde selectivity due to disproportionation reaction, resulting in the formation of toluene, reaching a maximum of approximately 2% with the monometallic 1wt% Pd/TiO_2.

Table 2. The catalytic performance of the prepared systems containing various Pd contents in benzyl alcohol oxidation. The reaction includes 0.02 g catalyst and 2 gm of benzyl alcohol conducted at 120 °C, O_2 (1 bar), stirred at 1000 rpm for 2 h.

Catalyst	Conversion %	Selectivity to Benzaldehyde %	TON [a]	TOF (h^{-1}) [b]
Pd/TiO_2	92.2	88.3	193.02	196.51
Cu/TiO_2	1.1	99.9	0.354	0.708
0.75Pd-0.25Cu/TiO_2	92.7	96.2	131.91	263.81
0.25Pd-0.75Cu/TiO_2	11.4	98.2	98.90	49.43
0.5Pd-0.5Cu/TiO_2	59.9	98.7	227.30	113.65

[a] TON = mmol of converted benzyl alcohol/mmol active species. [b] TOF = TON/time of reaction.

3.2.2. Effect of Temperature

To further determine the effect of temperature, a solvent-free benzyl alcohol reaction was performed with Cu–Pd/TiO_2 (1%) at 25, 50, 100, 110, 120, and 130 °C for 2 h in 1:1 mole ratio under aerobic conditions (1 bar of O_2). Table 3 shows the selectivity data of benzyl alcohol oxidation for six different reaction temperatures used. It is evident that a rise in temperature leads to a significant rise in the conversion of benzyl alcohol reaction. Also, there is a decrease in benzaldehyde selectivity with increasing temperature. On the other hand, there is an increase in toluene selectivity with increasing temperature. This may be explained by a previous study, which showed that low temperatures do not support disproportionation reactions. Moreover, these reactions increase with an increase in temperature [19].

Table 3. Effect of temperature on benzyl alcohol oxidation using 1%Cu–Pd/support with 1:1 mole ratio catalyst.

Temperature °C	Conversion %	Selectivity %	
		Benzaldehyde	Toluene
50	3.3	44.2	0.08
80	8.5	66.6	0.12
100	12.9	99.1	0.3
110	26.1	98.7	0.7
120	35.9	98.7	1
130	67.1	96.6	2.9

The reaction includes 0.02 g catalyst and 2 gm of benzyl alcohol conducted at O_2 (1 bar), stirred at 1000 rpm for 2 h.

3.2.3. Time Study

Effect of reaction time for benzyl alcohol reaction, under aerobic conditions (1 bar of O_2) was also determined using the 0.5%Cu-0.5%Pd/TiO_2 with 1:1 mole ratio catalyst under optimal conditions, which is shown in Figure 5. The conversion steadily increased with an increase in reaction time under these conditions. Deactivation of the catalysts was not observed in this reaction, although it is worth noting that this was at lower conversions. However, there was no effect of the reaction time leading to any variations in the selectivity of the products with increasing conversion. This clearly suggests that reaction pathways were operating in parallel.

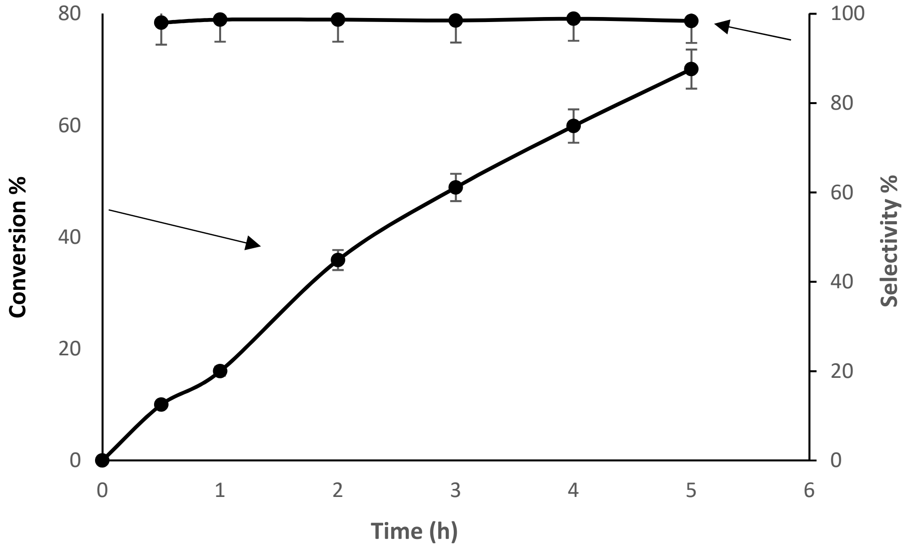

Figure 5. Effect of reaction time on the conversion of benzyl alcohol oxidation. The reaction includes 0.02 g catalyst and 2 gm of benzyl alcohol conducted at 120 °C, O_2 (1 bar), stirred at 1000 rpm.

3.2.4. Catalyst Reusability

Reusability profile of benzyl alcohol reaction, under aerobic conditions (1 bar of O_2), was determined using Pd–Cu/TiO_2 with 1:1 mole ratio catalyst under optimal conditions as shown in Figure 6. An increased activity was evident with fresh catalysts in comparison to first and second runs. The decrease in the catalytic performance could be due to the development of aggregated metallic nanoparticles (Cu and Pd) on the TiO_2 surface, along with the probability of Pd and Cu NPs leaching into the reaction mixture. We tested the leaching process of Pd–Cu/TiO_2 catalyst for benzyl alcohol oxidation. The Pd and Cu contents was estimated using ICP-OES before and after the second run. The quantitative results showed that the catalyst had a significant amount of Pd leaching (11%) from the beginning Pd concentration.

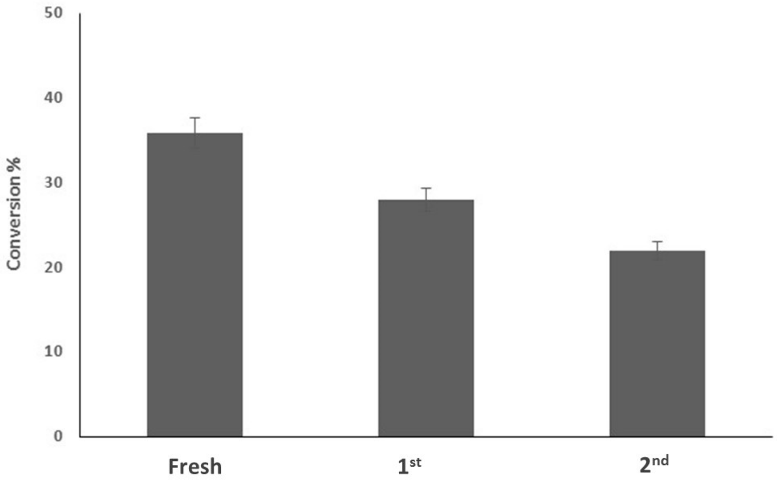

Figure 6. Conversion of benzyl alcohol during oxidation with reusability over Pd–Cu/TiO_2. Reaction conditions: 0.02 g catalyst and 2 gm of benzyl alcohol conducted at 120 °C, O_2 (1 bar), stirred at 1000 rpm.

Finally, as shown in Table 4, the bimetallic integration of copper with palladium supported on TiO_2 displayed the best activity in the benzyl alcohol oxidation when compared to other previously cited catalytic systems [35–38].

Table 4. Comparison of the benzyl alcohol oxidation activity over different catalysts.

Catalyst	Conversion %	Selectivity to Benzaldehyde %	Ref.
Au-Pd/TiO_2	51.7	76.71	[38]
Au-Pd/TiO_2	16	99	[39]
Au@Pd(0.049)/TiO_2	14.3	91.6	[40]
1Au1Pd/APS-S16	15.5	94	[41]
Pd–Cu/TiO_2	35.9	98.7	This work

4. Conclusions

One-percent Pd–Cu was synthesized using the sol-immobilization method over supports (TiO_2), and examined for the oxidation of benzyl alcohol to benzaldehyde. The results indicate that monometallic Cu/TiO_2 was observed to have a low activity. However, as soon as the catalyst contained any palladium, the activity increased, with a significant increase in selectivity towards isomerization products. The results indicate that a high initial activity for freshly prepared catalysts. The activity declined rapidly with number of runs, which could imply sintering of the support, or agglomeration and leaching of active phase. This study has provided insight in understanding how surface morphologies affect catalysts' activity and stability after several runs.

Supplementary Materials: The following are available online at https://www.mdpi.com/article/10.3390/pr9091590/s1, Section S1. GC data.

Funding: This research received no external funding.

Institutional Review Board Statement: Not applicable.

Informed Consent Statement: Not applicable.

Data Availability Statement: Not applicable.

Conflicts of Interest: The authors declare no conflict of interest.

References

1. Jachuck, R.J.J.; Selvaraj, D.K.; Varma, R.S. Process intensification: Oxidation of benzyl alcohol using a continuous isothermal reactor under microwave irradiation. *Green Chem.* **2006**, *8*, 29–33. [CrossRef]
2. Ragupathi, C.; Judith Vijaya, J.; Narayanan, S.; Jesudoss, S.K.; John Kennedy, L. Highly selective oxidation of benzyl alcohol to benzaldehyde with hydrogen peroxide by cobalt aluminate catalysis: A comparison of conventional and microwave methods. *Ceram. Int.* **2015**, *41*, 2069–2080. [CrossRef]
3. Ndolomingo, M.J.; Meijboom, R. Selective liquid phase oxidation of benzyl alcohol to benzaldehyde by tert-butyl hydroperoxide over gamma-Al_2O_3 supported copper and gold nanoparticles. *Appl. Surf. Sci.* **2017**, *398*, 19–32. [CrossRef]
4. Zhu, S.; Cen, Y.; Yang, M.; Guo, J.; Chen, C.; Wang, J.; Fan, W. Probing the intrinsic active sites of modified graphene oxide for aerobic benzylic alcohol oxidation. *Appl. Catal. B Environ.* **2017**, *211*, 89–97. [CrossRef]
5. Sheldon, R.A.; van Bekkum, H. *Fine Chemicals Through Heterogeneous Catalysis*; John Wiley & Sons Inc.: Hoboken, NJ, USA, 2001.
6. Enache, D.I.; Edwards, J.K.; Landon, P.; Solsona-Espriu, B.; Carley, A.F.; Herzing, A.A.; Watanabe, M.; Kiely, C.J.; Knightand, D.W.; Hutchings, G.J. Solvent-free oxidation of primary alcohols to aldehydes using Au-Pd/TiO_2 catalyst. *Science* **2006**, *311*, 362–365. [CrossRef]
7. Yamaguchi, K.; Mizuno, N. Supported ruthenium catalyst for the heterogeneous oxidation of alcohols with molecular oxygen. *Angew. Chem. Int. Ed. Engl.* **2002**, *41*, 4538–4542. [CrossRef]
8. Karimi, B.; Biglari, A.; Clark, J.H.; Budarin, V. Green, transition-metal-free aerobic oxidation of alcohols using a highly durable supported organocatalyst. *Angew. Chem. Int. Ed. Engl.* **2007**, *46*, 7210–7213. [CrossRef] [PubMed]
9. Hudlicky, M. *Oxidation in Organic Chemistry*; American Chemical Society: Washington, DC, USA, 1990.

10. Miyamura, H.; Matsubara, R.; Miyazaki, Y.; Kobayashi, S. Aerobic oxidation of alcohols at room temperature and atmospheric conditions catalyzed by reusable gold nanoclusters stabilized by the benzene rings of polystyrene derivatives. *Angew. Chem. Int. Ed. Engl.* **2007**, *46*, 4151–4154. [CrossRef]
11. Mahmood, A.; Robinson, G.E.; Powell, L. An improved oxidation of an alcohol using aqueous permanganate and phase-transfer catalyst. *Organ. Proc. Res. Dev.* **1999**, *3*, 363–364. [CrossRef]
12. Thottathil, J.K.; Moniot, J.L.; Mueller, R.H.; Wong, M.K.; Kissick, T.P. Conversion of L-pyroglutamic acid to 4-alkyl-substituted L-prolines. The synthesis of trans-4-cyclohexyl-L-proline. *J. Organ. Chem.* **1986**, *51*, 3140–3143. [CrossRef]
13. Bäckvall, J.-E. *Modern Oxidation Methods*; Wiley-VCH Verlag GmbH & Co. KGaA: Hoboken, NJ, USA, 2010.
14. Tojo, G.; Fernandez, M. *Oxidation of Alcohols to Aldehydes and Ketones*; Springer: Berlin/Heidelberg, Germany, 2006.
15. Ryland, B.L.; Stahl, S.S. Practical Aerobic Oxidations of Alcohols and Amines with Homogeneous Copper/TEMPO and Related Catalyst Systems. *Angew. Chem. Int. Ed.* **2014**, *53*, 8824–8838. [CrossRef]
16. Villa, A.; Wang, D.; Dimitratos, N.; Su, D.; Trevisan, V.; Prati, L. Pd on carbon nanotubes for liquid phase alcohol oxidation. *Catal. Today* **2010**, *150*, 8–15. [CrossRef]
17. Liu, J.; Zou, S.; Lu, L.; Zhao, H.; Xiao, L.; Fan, J. Room temperature selective oxidation of benzyl alcohol under base-free aqueous conditions on Pt/TiO_2. *Catal. Commun.* **2017**, *99*, 6–9. [CrossRef]
18. Albadi, J.; Alihoseinzadeh, A.; Razeghi, A. Novel metal oxide nanocomposite of Au/CuO-ZnO for recyclable catalytic aerobic oxidation of alcohols in water. *Catal. Commun.* **2014**, *49*, 1–5. [CrossRef]
19. Zhan, G.; Huang, J.; Du, M.; Sun, D.; Abdul-Rauf, I.; Lin, W.; Hong, Y.; Li, Q. Liquid phase oxidation of benzyl alcohol to benzaldehyde with novel uncalcined bioreduction au catalysts: High activity and durability. *Chem. Eng. J.* **2012**, *187*, 232–238. [CrossRef]
20. Ganesamoorthy, S.; Tamizh, M.M.; Shanmugasundaram, K.; Karvembu, R. Immobilization of Ru (III) complex on silica: A heterogenized catalyst for selective oxidation of alcohols in water at room temperature. *Tetrahedron Lett.* **2013**, *54*, 7035–7039. [CrossRef]
21. Friend, C.M.; Xu, B. Heterogeneous Catalysis: A Central Science for a Sustainable Future. *Acc. Chem. Res.* **2017**, *50*, 517–521. [CrossRef] [PubMed]
22. Nishimura, S. *Handbook of Heterogeneous Catalytic Hydrogenation for Organic Synthesis*; Wiley: New York, NY, USA, 2001.
23. Astruc, D. *Nanoparticles and Catalysis*; Wiley: New York, NY, USA, 2008. [CrossRef]
24. Bilgicli, H.G.; Burhan, H.; Diler, F.; Cellat, K.; Kuyuldar, E.; Zengin, M.; Sen, F. Composites of palladium nanoparticles and graphene oxide as a highly active and reusable catalyst for the hydrogenation of nitroarenes. *Microporous Mesoporous Mater.* **2020**, *296*, 110014. [CrossRef]
25. Dilera, F.; Burhan, H.; Genca, H.; Kuyuldarb, E.; Zengin, M.; Cellat, K.; Senb, F. Efficient preparation and application of monodisperse palladium loaded graphene oxide as a reusable and effective heterogeneous catalyst for suzuki cross-coupling reaction. *J. Mol. Liq.* **2020**, *298*, 111967. [CrossRef]
26. Kakiuchi, N.; Maeda, Y.; Nishimura, T. Uemura, S. Pd(II)−Hydrotalcite-Catalyzed Oxidation of Alcohols to Aldehydes and Ketones Using Atmospheric Pressure of Air. *J. Org. Chem.* **2001**, *66*, 6620–6625. [CrossRef]
27. Chan-Thaw, C.E.; Savara, A.; Villa, A. Selective benzyl alcohol oxidation over Pd catalysts. *Catalysts* **2018**, *8*, 431. [CrossRef]
28. Yang, C.-C.; Yu, Y.-H.; van der Linden, B.; Wu, J.C.S.; Mul, G. Artificial photosynthesis over crystalline TiO_2-based catalysts: Fact or fiction? *J. Am. Chem. Soc.* **2010**, *132*, 8398–8406. [CrossRef]
29. Pelton, R.; Geng, X.; Brook, M. Photocatalytic paper from colloidal TiO_2-fact or fantasy. *Adv. Colloid Interface Sci.* **2006**, *127*, 43–53. [CrossRef] [PubMed]
30. Saikia, H.; Borah, B.J.; Yamada, Y.; Bharali, P. Enhanced catalytic activity of CuPd alloy nanoparticles towards reduction of nitroaromatics and hexavalent chromium. *J. Colloid Interface Sci.* **2017**, *486*, 46–57. [CrossRef]
31. Diyarbakir, S.; Can, H.; Metin, Ö. Reduced Graphene Oxide-Supported CuPd Alloy Nanoparticles as Efficient Catalysts for the Sonogashira Cross-Coupling Reactions. *ACS Appl. Mater. Interfaces* **2015**, *7*, 3199–3206. [CrossRef] [PubMed]
32. Nasrollahzadeh, M.; Jaleh, B.; Ehsani, A. Preparation of carbon supported CuPd nanoparticles as novel heterogeneous catalysts for the reduction of nitroarenes and the phosphine-free Suzuki–Miyaura coupling reaction. *New J. Chem.* **2015**, *39*, 1148–1153. [CrossRef]
33. Zamaraev, K.I. Catalytic science and technology for environmental issues. *Catal. Today* **1997**, *35*, 3–13. [CrossRef]
34. Kluson, P.; Cerveny, L. Selective hydrogenation over ruthenium catalysts. *Appl. Catal. A Gen.* **1995**, *128*, 13–31. [CrossRef]
35. Kim, K.S.; Gossmann, A.F.; Winograd, N. X-ray photoelectron spectroscopic studies of palladium oxides and the palladium-oxygen electrode. *Anal. Chem.* **1974**, *46*, 197–200. [CrossRef]
36. Mukherjee, P.; Roy, P.S.; Mandal, K.; Bhattacharjee, D.; Dasgupta, S.; Bhattacharya, S.K. Improved catalysis of room temperature synthesized Pd-Cu alloy nanoparticles for anodic oxidation of ethanol in alkaline media. *Electrochim. Acta* **2015**, *154*, 447–455. [CrossRef]
37. Zhang, L.; Persaud, R.; Madey, T.E. Ultrathin metal films on a metal oxide surface: Growth of Au on TiO_2 (110). *Phys. Rev. B* **1997**, *56*, 10549–10557. [CrossRef]
38. Li, X.; Feng, J.; Sun, J.; Wang, Z.; Zhao, W. Solvent-Free Catalytic Oxidation of Benzyl Alcohol over Au-Pd Bimetal Deposited on TiO_2: Comparison of Rutile, Brookite, and Anatase. *Nanoscale Res. Lett.* **2019**, *14*, 394. [CrossRef]

39. Zhan, B.Z.; White, M.A.; Sham, T.K.; Pincock, J.A.; Doucet, R.J.; Rao, K.V.R.; Robertson, K.N.; Cameron, T.S.J. Zeolite-confined nano-RuO_2: A green, selective, and efficient catalyst for aerobic alcohol oxidation. *Am. Chem. Soc.* **2003**, *125*, 2195. [CrossRef] [PubMed]
40. Sun, J.; Han, Y.; Fu, H.; Qu, X.; Xu, Z.; Zheng, S. Au@ Pd/TiO_2 with atomically dispersed Pd as highly active catalyst for solvent-free aerobic oxidation of benzyl alcohol. *Chem. Eng. J.* **2017**, *313*, 1–9. [CrossRef]
41. Chen, Y.; Lim, H.; Tang, Q.; Gao, Y.; Sun, T.; Yan, Q.; Yang, Y. Solvent-free aerobic oxidation of benzyl alcohol over Pd monometallic and Au–Pd bimetallic catalysts supported on SBA-16 mesoporous molecular sieves. *Appl. Catal. A Gen.* **2010**, *380*, 55–65. [CrossRef]